

Background Noise Reduction with a Fabry-Perot Etalon Filter in the HARLIE System

Sangwoo Lee and David O. Miller
Science System Applications Inc.
5900 Princess Garden Parkway suite 300
Lanham MD, 20706

Geary Schwemmer
Laboratory for Atmosphere, Code 912
NASA Goddard Space Flight Center
Greenbelt, MD 20771

1. INTRODUCTION

Background noise reduction of lidar signals is one of the most important factors in achieving better signal to noise ratio and precise atmospheric data from lidar measurements. Fabry Perot etalons have been used in several lidar systems as narrow band pass filters in the reduction of scattered sunlight¹. An etalon with spectral bandwidth, $\Delta\nu=0.23\text{ cm}^{-1}$, free spectral range, $\text{FSR}=6.7\text{ cm}^{-1}$, and diameter, $d=24\text{mm}$ was installed in a fiber coupled box which included a 500 pm bandwidth interference filter. The etalon box couples the telescope and detector with 200 μm core fibers and 21 mm focal length collimators. The angular magnification is $M=48$. The etalon box was inserted into the Holographic Airborne Rotating Lidar Instrument Experiment (HARLIE) system² and tested during the HARGLO-2 intercomparison campaign conducted in November 2001 at Wallops Island, Virginia. This paper presents the preliminary test results of the etalon and a complete analysis will be presented at the conference.

2. EXPERIMENTAL SETUP

Employing a 360-degree scanning holographic optical element (HOE) as a telescope lens, HARLIE is a backscatter lidar system capable of measuring aerosol distributions, wind velocity and direction measurements, and cloud and boundary layer heights. HARLIE is composed of a diode-pumped Nd:YAG laser with a 5 kHz repetition rate, a receiver system with a 40 cm transmission HOE, a photon counting detector and a data acquisition system accumulating and storing data at 100 ms intervals with 100 ns range bins. Figure 1 shows the schematic diagram of the lidar system.

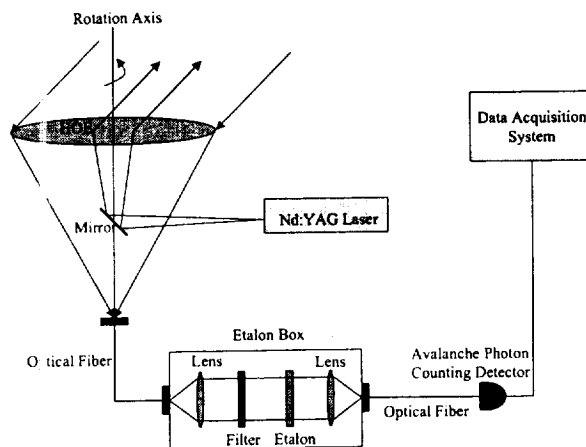


Figure 1. The schematic diagram of HARLIE system with the etalon box

The HOE diffracts the outgoing laser beam 45 degrees and collimates the beam to 150 micro-radians. It also focuses the backscattered signal from the atmosphere onto a 200 μ m optical fiber. The etalon box consists of a fiber collimating lens, the etalon, and an interference filter, and focusing lens. A second optical fiber sends the light signal to a photon counting avalanche photodiode. The temperature of the etalon box is stabilized above ambient using a temperature controller.

3. EXPERIMENTS AND DATA ANALYSIS

Lidar backscatter data was taken with and without the etalon box during daytime. Collected data was stored for post processing analysis. Figure 2 is the image of the signal with and without the etalon. The system was operated without the etalon during the first half of the data set and with the etalon during the last half of the data. The area in the middle of the image corresponds to a break period for the etalon installation.

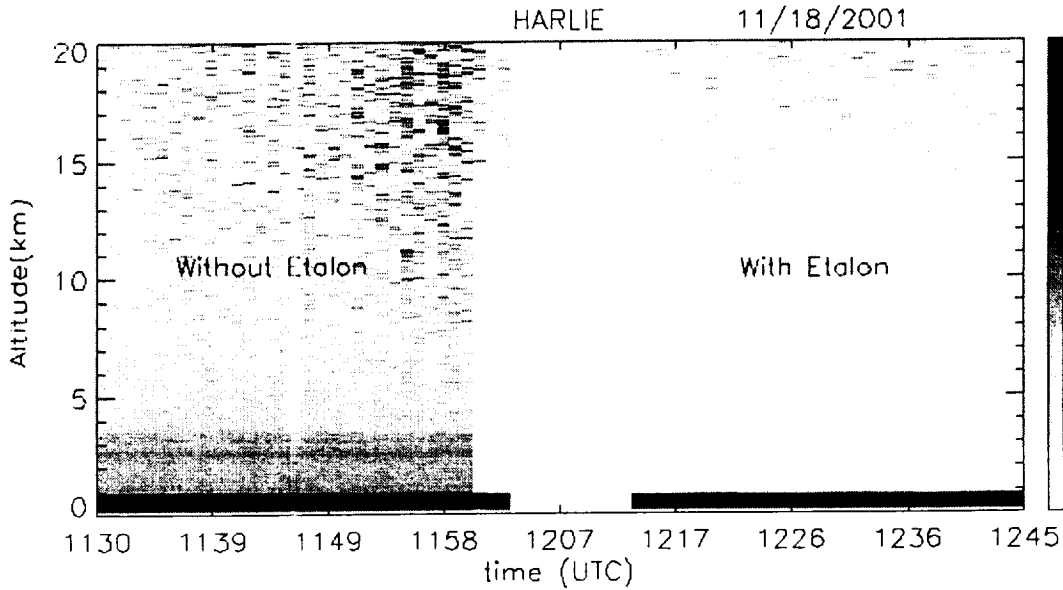


Figure 2. The image of the lidar signal with and without the etalon.

The measured signal can be expressed by this simple form of the lidar equation³, $V(z)$,

$$V(z) = \frac{C \cdot E_o \cdot \beta(z) \cdot T^2(z)}{z^2} + b \quad (1)$$

where $V(z)$ is the measured signal from altitude z , C is the lidar system calibration factor, E_o is the Transmitted pulse energy, $\beta(z)$ is the volume backscatter coefficient of the atmosphere at altitude z , T is the atmospheric transmittance and b is the background signal level. For both signals with and without the etalon, the measured values of the parameters in the expression should be the same except for the system calibration factor and the background level by assuming atmospheric change is negligible during the experiment. Therefore, the signal for the system with the etalon can be simply given by replacing C and b with C_{etalon} and b_{etalon} in the equation. After subtracting the background, the ratio of the signal with the etalon to the signal without the etalon should be a constant, α ,

$$\alpha = \frac{V_{etalon}(z) - b_{etalon}}{V(z) - b} = \frac{S_{etalon}(z)}{S(z)} = \frac{C_{etalon}}{C} \quad (2)$$

where the lidar backscatter portions of the signals are substituted with $S(z)$. By comparing the ratio of the calibration factors and the background levels, we can determine the performance of the etalon. Figure 3(a) is a plot of a 30-minute average of backscattered signals without and with the etalon. The raw signals were first corrected for pulse pile-up (detector dead-time). Then the background level was subtracted. The background level was obtained by averaging over the last 100 bins of the signal, corresponding to 18-20 km altitude. Figure 3(b) shows the ratio of the signal with the etalon to the signal without the etalon. Using Poisson statistics, the noise in the backscattered signals,

$$S_j(z) = V_j(z) - b_j \quad (3)$$

is given by

$$N_j(z) = \sqrt{V_j(z) + b_j} \quad (4)$$

where j represents with or without the etalon. Therefore the signal to noise ratio is computed as,

$$\frac{S}{N} = \frac{S_j(z)}{\sqrt{V_j(z) + b_j}} \quad (5)$$

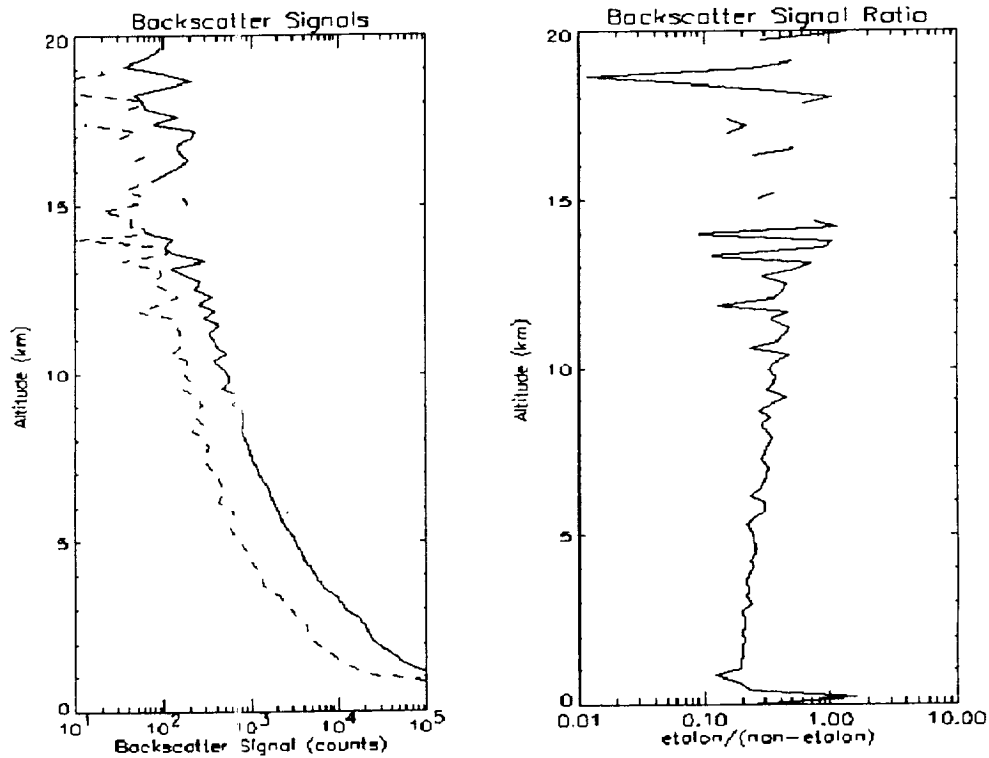


Figure 3. (a). The background-subtracted backscattered signals. The broken line is the signal with the etalon and the solid line is the signal without the etalon. (b). The backscatter ratio of the signal with etalon to the signal without etalon.

4. DISCUSSION

The 30-minute background levels are 4790 and 820 counts/range bin for the signal without and with the etalon, respectively. The noises and the signal to noise ratio are calculated by using equation (4). The background level with the etalon is about 6 times smaller than the one without. The signals, noise, and the signal to noise ratio at several different altitudes are listed in table 1. The etalon decreases the signal to noise ratio of the system by factor 2 at lower altitudes, to a factor of 1 at higher altitudes. As we can see in figure 3(b), the backscatter ratio of the signal with the etalon to the signal without the etalon gradually changes as a function of altitude. This might be explained by the fact that backscattered signals from different ranges will have different angular extent, hence will be collimated to differing degrees by the collimating lens in the etalon box. This will have an effect on the transmission of the etalon.

Altitude (km)	Raw Signal, S (Counts)	Noise, N (Counts)	S/N	Raw Signal, S _{etalon} (Counts)	Noise, N _{etalon} (Counts)	S _{etalon} /N _{etalon}	(S _{etalon} /N _{etalon})/(S/N)
2	28000	181	155	6000	83	72	0.46
4	5200	100	52	1100	44	25	0.48
6	2000	82	24	550	37	15	0.63
8	920	76	12	290	33	9	0.75
10	490	73	7	180	31	6	0.86
12	300	71	4	120	30	4	1

Table 1. The signals, noise, and the signal to noise ratio at several different altitudes without and with the etalon, calculated for 30-minute integrations and 100 ns range gates.

5. CONCLUSION

An etalon as a narrow band pass filter was inserted into the HARLIE system and tested. The etalon did not improve the signal to noise ratio of the HARLIE data for the data set presented. This may be due to a number of things. One is a changing background light level during the experiment. Another is the decreased etalon transmission due to a combination of higher divergence of the near field signals and the finite spectral bandwidth of the laser. The etalon transmission at higher altitudes approaches our lab measured peak transmission of 60%, but the background levels do not agree with the predicted spectral rejection, reaching a factor of 3.5 reduction in spectral bandwidth after correcting for the peak transmission, instead of the expected factor of 20 reduction. The range dependence of the signal ratio has information, which may be used to determine the laser divergence, but the spectral characteristics of the laser must be known. We will be independently characterizing the spectral and divergence properties of the laser in order to determine if the field measurements verify the expected performance of the narrowband etalon as a background rejection filter.

REFERENCES

1. Li, Steven X., Bruce M. Gentry, C. Laurance Korb, Savyasachee Mathur, and Huailin Chen, "Capacitively stabilized etalon technology for spaceborne wind lidar application," 19th International Laser Radar Conference, pp 915-918, 1998.
2. Schwemmer, Geary, Thomas Wilkerson, and David Guerra, "Compact scanning lidar systems using holographic optics," Proceedings of SPIE Vol. 3504, pp 51-59, 1998.
3. Reagan, John A., M. Patrick McCormick, and James D. Spinhirne, "Lidar sensing of aerosols and clouds in the troposphere and stratosphere," Proceedings of the IEEE, vol. 77, No. 3, pp 433-448, March 1989.

HARLIE 3-D Aerosol Backscatter and Wind Profile Measurements During Recent Field Experiments

Geary K. Schwemmer^{*a}, Thomas D. Wilkerson^c, David O. Miller^b, Ionio Andrus^c, Cameron Egbert^c,
Mark Anderson^c, Sangwoo Lee^b

^aLaboratory for Atmospheres, NASA Goddard Space Flight Center; ^bScience Systems and Applications
Inc., ^cUtah State University

ABSTRACT

We report scanning lidar measurement results from several field campaigns in which the Holographic Airborne Rotating Lidar Instrument Experiment (HARLIE) was used in a ground-based, upward-looking mode to map time-resolved, 3-D aerosol profiles. Horizontal wind vectors are derived from analysis of the aerosol data using two techniques that quantify backscatter structure motion across the scan. Measurements were made at the Department of Energy-Atmospheric Radiation Measurement (ARM-DoE) site in Oklahoma during the Water Vapor Intensive Operating Period in September/October 2000 and during the HARGLO-1 and HARGLO-2 wind measurement intercomparisons with the Goddard Lidar Observatory Winds (GLOW) in Greenbelt, Maryland and Wallops Island, Virginia, respectively. Two novel algorithms facilitate the wind vector analysis of HARLIE data. Observed wind velocity and direction are compared with wind measurements from radiosonde, Doppler lidar, Doppler radar and cloud track winds. The results demonstrate good agreement between HARLIE data and data from the other measurements. The conically scanning holographic lidar opens up new possibilities for obtaining the vertical profile of horizontal winds.

Keywords: lidar, backscatter, atmospheric aerosols, clouds, holographic optical element, scanning, atmospheric dynamics, Doppler, wind profiles, scanning lidar, HARLIE, AROL-2, GLOW, cloud tracking, holographic lidar

1. INTRODUCTION

Holographic scanning lidar is a new technology for replacing large aperture scanning telescope systems with lighter, less costly, and simpler optical mechanisms. This is seen as an enabling technology for the eventual use of scanning lidars in spaceborne Earth remote sensing instruments. It is based on the use of large Holographic Optical Elements (HOEs) to collimate and transmit laser light as well as collect and focus atmospheric backscatter while scanning in a conical pattern.¹ Conical scanning is perhaps the most efficient means of obtaining multiple look angles and cross track coverage. There are many applications: topographic mapping, 3-D atmospheric aerosol and cloud structures², and wind profiling based on the motions of backscatter structures³⁻⁷ or by combining the holographic scanning telescope with a Doppler lidar receiver.

The HARLIE⁸ scanning HOE produces a 45-degree conical scan. For ground-based observations, we typically use a scan rate of 10 degrees/sec to enhance azimuth angular resolution. A 1064 nm wavelength Nd:YAG laser transmits 1-mJ Q-switched pulses at a 5 KHz repetition rate. Shots are accumulated using multi-channel scalars with photon-counting detectors. 100-ms integration times yields an atmospheric profile for every 1-degree in azimuth. The range resolution is 30 meters, corresponding to 20 meters in altitude resolution for the 45-degree fixed elevation angle. The backscatter data obtained from a stationary (i.e. ground-based) location, when viewed over many consecutive scans, reveals atmospheric motions over a conical surface as the atmosphere advects over the site.

During previous field experiments^{9,10} involving HARLIE ground-based measurements in concert with a zenith wide-angle video camera (SKYCAM), the Army Research Office Lidar 2 (AROL-2), and the Prototype Holographic Atmospheric Scanner for Environmental Remote Sensing¹¹ we developed methods for obtaining wind profiles from HARLIE data and from the SKYCAM video recordings; combining with AROL-2 measured cloud altitudes. The objectives for deploying HARLIE in the WVIOP were to test a new trailer configuration for ground based deployments, acquire data sets with coincident rawinsondes for validating our wind profile algorithms, and to obtain simultaneous Raman lidar measurements for transferring absolute backscatter calibration information. Based on the success of the HOLO and ARM field experiments, a series of wind measurement intercomparisons between HARLIE and GLOW, named HARGLO, were started.

* geary.schwemmer@gsfc.nasa.gov; phone 301-614-5768; fax 301-614-5492; Code 912, NASA Goddard Space Flight Center, Greenbelt, MD, USA 20771

2. ARM WATER VAPOR INTENSIVE OPERATING PERIOD (WVIOP) 2000

The WVIOP 2000 ran from 18 September through 8 October, 2000 at the DoE Climate and Radiation Test-bed (CART) site near Lamont, Oklahoma. Part of the Great Plains, the area is flat, semi-arid pasture and grain farmland, criss-crossed by a grid of dirt roads. For this deployment, we integrated HARLIE into a highly portable, 2.5x4.4 meter trailer for ease in transport and field operations. Installed in the rear of the trailer, HARLIE is positioned so the HOE is facing up and only a few centimeters from a transmitting window in the roof. The forward portion of the trailer houses the electronics rack, desk, and workspace for an operator, if required. The entire system can be set up after transporting to the deployment site in about one hour, and then is operated autonomously. A small X-band scanning radar probes the sky for aircraft and shutsters the laser whenever they approach HARLIE airspace. The wide-angle SKYCAM cloud video camera was set up outside the trailer on a tripod, and being a visible-light color camera, its use is restricted to daytime, non-precipitating conditions. For HARGLO, SKYCAM was installed in a weather-tight enclosure. We used cloud altitudes from the HARLIE data to combine with the angular motions of cloud features from the SKYCAM videos to generate independent cloud-tracked wind profiles. The ARM program launched rawinsondes every three hours, which we used for independent wind profile comparisons with both the HARLIE wind profiles and the SKYCAM wind profiles. HARLIE recorded over 110 hours of data on 16 days during WVIOP.

3. HARGLO WIND LIDAR INTERCOMPARISONS

The first intensive inter-comparison of HARLIE wind measurements with the GLOW Doppler Lidar was carried out over 15-20 November 2001 at Wallops Island, Virginia. Preceded by a warm-up series of measurements at Goddard dubbed HARGLO-1, HARGLO-2 included simultaneous and co-located wind measurements from rawinsondes, SKYCAM, and the SPANDAR Doppler radar. Both the lidars and SPANDAR scanned the sky in a conical mode with a 45-degree elevation angle. HARLIE being a 1-micron backscatter lidar, and GLOW being a UV Doppler lidar, take complementary data; HARLIE obtaining its measurements under high aerosol loading and GLOW obtaining its best measurements in clear air using the Rayleigh backscatter from molecules.

Briefly, the objectives of HARGLO-2 were to: 1) Perform an inter-comparison of wind profile data between HARLIE, GLOW, and other wind measuring instruments; 2) Explore and assess the range of overlap of HARLIE and GLOW data as a function of atmospheric conditions; 3) Develop an operational and scientific capability towards future calibration/validation of spaceborne DWL; 4) Compare the results of the two methods of processing HARLIE data to retrieve wind vector profiles.

GPS rawinsondes were launched at 1500 and 2000UT each day from a location about 2 km east of the lidar location. National Weather Service sondes, which use the LORAN location system to calculate winds, are launched daily at 1100 and 2300 UT at the NASA Wallops airfield about 10 km to the northeast. On the last day, a GPS sonde was launched simultaneously (but not co-located) at 2300 on 19 November so we could compare differences between sonde measurements due to the distance between launch sites. Being in-situ point sensors, they are subject to the whims of turbulent eddies in the atmosphere as they ascend, and may not always be an adequate representation of the mean wind over larger air parcels, of the size of future spaceborne DWL measurement sample volumes. Examining the sampling issues of the various wind instruments to a range of atmospheric spatial and temporal scales will be a goal of this and future DWL cal/val exercises.

4. HARLIE WINDS

Atmospheric motions are most easily visualized with a series of polar plot backscatter images similar to the one in Fig. 1 where the radial axis represents range in km. For HARLIE's 45-degree elevation angle, the horizontal distance from the lidar is also equal to the altitude. A time series of these images can be displayed sequentially on a computer screen as an animated sequence that can be used to help interpret atmospheric dynamic activity.

We have developed two techniques for deriving horizontal wind vectors from the HARLIE data, one graphical, and one numerical. The graphical method is best understood by referring to Fig. 2. Adopting a space-time diagrammatic technique used in studies of hydrodynamic waves, we image the lidar signals at one particular altitude interval in azimuth-time space. This "wave image" of the cloud field above the lidar site will have a characteristic pattern from which the flow parameters, i.e. wind direction and velocity, can be derived, either from a curve fit to the arccosine function or from the position and value of the slopes of that curve at its inflection points. The superimposed curve and straight-line slope are fit to the patterns

using an interactive graphical user interface, and provide the velocity (from the amplitude of the arccosine) and direction (from the phase) of the wind.

Figure 3 is a plot of HARLIE wind speed (left) and direction (right) measurements (shaded symbols with error bars) retrieved using the graphical data reduction technique just described. The HARLIE winds are compared with rawinsonde-derived winds (black diamonds) during HARGLO-2. The error bars on the HARLIE data represent the RMS of several measurements retrieved from a single wave image for a 30-minute period. Data are plotted from four consecutive 30-minute periods. HARLIE wind retrievals, relying on structure in the backscatter due to the presence of aerosols and clouds are usually grouped in and near the boundary layer and cloud layers. In general the agreement is quite good. When the differences in HARLIE and sonde data are more than ~ 3 m/s, we find that it usually occurs in areas of shear and turbulence, which often go hand in hand. The variance in sonde data is also largest in these regions. We are examining the occasional discrepancy such as the wind directions near 11 km in Fig. 4, occurring between 1430h and 1500h UT.

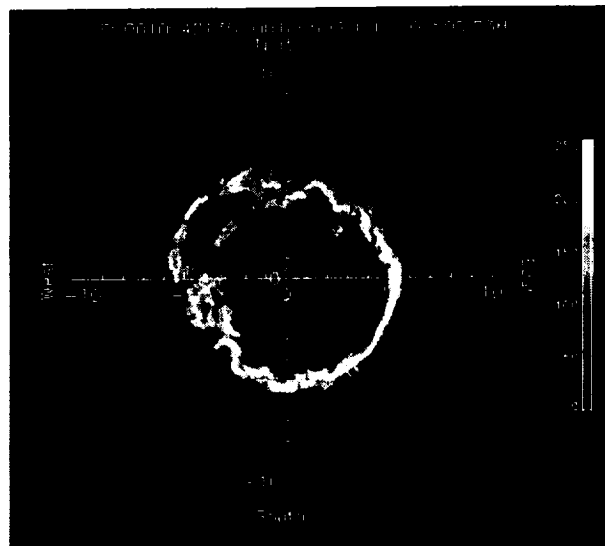
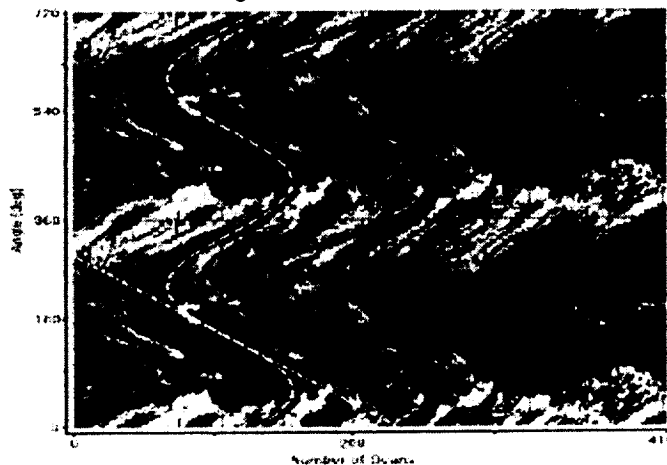


Figure 1. Polar plot of a single 36-sec scan of HARLIE data for 5 October 2000, at 0023h UT. Optically thin clouds are present in all directions, ranging in altitude from 2 to 6 km.

5. CONCLUSIONS AND PROSPECTS FOR FUTURE WORK

The conically scanning holographic lidar, HARLIE, has successfully been applied to the measurement of altitude profiles of wind velocity and direction, over altitudes ranging from 0.5 – 15 km and wind velocities up to 40 meters/second. The basic method is the *non-Doppler*, scanning lidar observation of the backscatter patterns of aerosols and clouds, using a novel kinematic data display and associated algorithms. In four measurement campaigns in Utah, New Hampshire, Oklahoma, and Virginia, HARLIE wind data were compared with independent data from radiosondes, from altitude-calibrated videos of cloud motion (AROL-2 and SkyCam), and from the GLOW Doppler lidar. The precisions of the HARLIE and AROL methods are in the range 0.5 – 2.0 meters/second. Comparisons of these two techniques demonstrate agreement to within ± 1.5 meters/second, for data pairs taken within five minutes of each other. In many instances HARLIE wind profiles are obtained over several altitudes at once, in spite of significant cloud cover. Good agreement with radiosonde wind records has been observed, considering that the time- and distance-dependence inherent in balloon observations makes rigorous comparisons difficult.

The instrumentation for future HARLIE measurement campaigns needs to be expanded to include other instantaneous profiling methods such as radar, Doppler lidar (both coherent and direct-detection), and radio-acoustic sounding. For the calibration and validation of lidar systems destined for aircraft and satellites, HARLIE will provide a unique source of comparison data. For general meteorological use, both at fixed and portable stations, HARLIE offers good prospects for efficient, affordable, round-the-clock profiling of winds wherever such data are needed. Automated data reduction methods are under development to facilitate expanded applications of the HARLIE method of wind profiling.



ACKNOWLEDGEMENTS

We acknowledge the generous support of this research by NASA, the Integrated Program Office of the NPOESS program, the Space Dynamics Laboratory of Utah State University, the Atmospheric Radiation Measurement program of the DoE.

REFERENCES

- Schwemmer, Geary K., and Thomas D. Wilkerson, "Holographic Optical Elements as Conically Scanned Lidar Telescopes," *Tech. Digest on Optical Remote Sensing of the Atmosphere*, (Optical Society of America, Wash. D. C.), Vol. 18, pp. 310-312, 1991.
- Schwemmer, G. K., D. O. Miller, T. D. Wilkerson, I. Q. Andrus, "Time Resolved 3-D mapping of atmospheric aerosols and clouds during the recent ARM Water Vapor IOP", *Proceedings of SPIE Vol. 4484 Optical Remote Sensing for Industry and Environment Monitoring II*, San Diego, California, 30-31 July 2001, pp. 58-63.
- Sroga, J.T. and E.W. Eloranta, "Lidar measurements of wind velocity profiles in the boundary layer," *J. Appl. Meteor.* **19**, pp. 598-605, 1980.
- Sasano Y., H. Hirohara, T. Yamasaki, H. Shimizu, N. Takeuchi and T. Kawamura, "Horizontal wind vector determination from the displacement of aerosol distribution patterns observed by a scanning lidar," *J. Appl. Meteor.* **21**, pp. 1516-1523, 1980.
- Pal, S. R., I. Pribluda and A.I. Carswell, "Lidar Measurements of Cloud-Tracked Winds," *J. Appl. Meteor.* **35**, 35-44, 1994.
- Sanders, J.A., *Lidar Tropospheric Wind Vector Measurements*, MS thesis, Department of Physics Utah State University, Logan, UT, 2000.
- Wilkerson, T. D., I. Q. Andrus, G. K. Schwemmer, D. O. Miller, "Horizontal Wind Measurements using the HARLIE Holographic Lidar", *Proceedings of SPIE Vol. 4484 Optical Remote Sensing for Industry and Environment Monitoring II*, San Diego, California, 30-31 July 2001, pp. 64-73.
- Schwemmer, G. K., "Holographic Airborne Rotating Lidar Instrument Experiment," *19th International Laser Radar Conference*, NASA/CP-1998-207671/PT2, pp. 623-626, Annapolis, Maryland, 6-10 July 1998.
- Wilkerson, T. D., J. A. Sanders, I. Q. Andrus, G. K. Schwemmer, D. O. Miller, D. V. Guerra, J. Schnick, and S. E. Moody, "The HOLO series: Critical ground-based demonstrations of holographic scanning lidars," *Proc. 2nd Asia-Pacific Symposium on Remote sensing*, Sendai, Japan, October 9-12, 2000, SPIE **4153**, pp. 63-69, 2001.
- Schwemmer, Geary K., Thomas D. Wilkerson, Jason A. Sanders, David V. Guerra, David O. Miller, Stephen E. Moody, "Ground Based Operational Testing of Holographic Scanning Lidars," *Advances in Laser Remote Sensing*, Alain Dabas, Claude Loth and Jacques Pelon, Editors, pp. 69-72, Ecole Polytechnique, publisher, France, 2001.
- Guerra, D. V., A. D. Wooten, Jr., S. S. Chaudhuri, G. K. Schwemmer, and T. D. Wilkerson, "Prototype Holographic Atmospheric Scanner for Environmental Remote Sensing", *J. Geophysical Research*, Vol. 104, No. D18, 22,287-22,292, 1999.

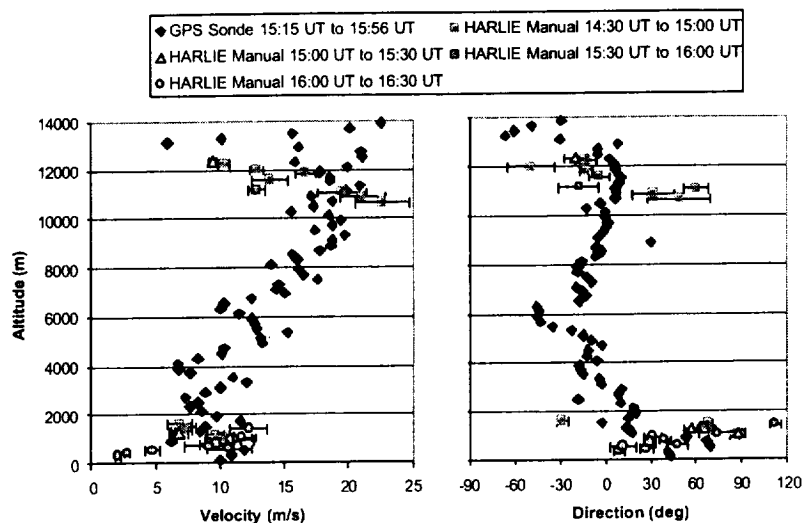


Figure 3. HARLIE wind speed (left) and direction (right) retrieved using the GUI method, compared with a rawinsonde profile (black diamonds) from HARGLO-2.